The Aging imageomics study: rationale, design and baseline characteristics of the study population

Puig, J.; Biarnes, C.; Pedraza, S.; Vilanova, J.C.; Pamplona, R.; Fernandez-Real, J.M.; ... ; Garre-Olmo, J.

Mechanisms of Ageing and Development 189 (2020) 111257

Contents lists available at ScienceDirect

Mechanisms of Ageing and Development

journal homepage: www.elsevier.com/locate/mechagedev

The Aging Imageomics Study: rationale, design and baseline characteristics of the study population

Josep Puig[a,b,c,d,*], Carles Biarnes[a,b], Salvador Pedraza[a,b,c], Joan C. Vilanova[a,b,c], Reinald Pamplona[e], José Manuel Fernández-Real[b,c,f], Ramon Brugada[b,c,g], Rafel Ramos[b,c,h,i,*], Gabriel Coll-de-Tuero[j,k,l], Laia Calvo-Perxas[b], Joaquin Serena[b,c,m], Lluís Ramió-Torrentà[b,c,m], Jordi Gich[b,m], Lluis Gallart[n], Manel Portero-Otin[e], Angel Alberich-Bayarri[o], Ana Jimenez-Pastor[o], Eduardo Camacho-Ramos[o], Jordi Mayneris-Perxachs[b,c,f], Victor Pineda[a,b], Raquel Font[p], Anna Prats-Puig[p], Mariano-Luis Gacto[p], Gustavo Deco[q,r], Anira Escrichs[q], Bonaventura Clotet[s,t,u], Roger Paredes[s,t,u], Eugenia Negredo[s,t,u], Bruno Triaire[v], Manuel Rodríguez[v], Alberto Heredia-Escámez[v], Rafael Coronado[v], Wolter de Graaf[v], Valentin Prevost[v], Anca Mitulescu[w], Pepus Daunis-i-Estadella[x], Santiago Thió-Henestrosa[x], Felip Miralles[y], Vicent Ribas-Ripoll[y], Manel Puig-Domingo[z], Marco Essig[d], Chase R. Figley[d], Teresa D. Figley[d], Benedict Albensi[aa], Ahmed Ashraf[bb], Johan H.C. Reiber[cc], Giovanni Schifitto[dd], Md Nasir Uddin[dd], Carlos Leiva-Salinas[ee], Max Wintermark[ff], Kambiz Nael[gg], Joan Vilalta-Franch[b,c,hh], Jordi Barretina[b], Josep Garre-Olmo[b,c,hh]

[a] *Department of Radiology (IDI), Hospital Universitari de Girona Dr Josep Trueta, Girona, Spain*
[b] *Girona Biomedical Research Institute (IDIBGI), Hospital Universitari de Girona Dr Josep Trueta, Girona, Spain*
[c] *Department of Medical Sciences, School of Medicine, University of Girona, Girona, Spain*
[d] *Department of Radiology, University of Manitoba, Winnipeg, MB, Canada*
[e] *Department of Experimental Medicine, Faculty of Medicine, University of Lleida-IRBLleida, Lleida, Spain*
[f] *Department of Diabetes, Endocrinology and Nutrition, IDIBGI, Hospital Universitari de Girona Dr Josep Trueta, CIBER Fisiopatología de la Obesidad y Nutrición (CIBERobn), Girona, Spain*
[g] *Cardiovascular Genetics Center, CIBER-CV, IDIBGI, Girona, Spain*
[h] *Vascular Health Research Group of Girona (ISV-Girona), Institut Universitari d'Investigació en Atenció Primària Jordi Gol (IDIAP Jordi Gol), Girona, Spain*
[i] *Primary Care Services, Catalan Institute of Health (ICS), Girona, Spain*
[j] *Research Support Unit, University Institute of Research in Primary Care JordiGol (IdIAPGol), Girona, Spain*
[k] *Research Group on Statistics, Econometrics and Health (GRECS), University of Girona, Girona, Spain*
[l] *CIBER of Epidemiology and Public Health (CIBERESP), Madrid, Spain*
[m] *Department of Neurology, Hospital Universitari de Girona Dr Josep Trueta, Girona, Spain*
[n] *Biobanc, Girona Biomedical Research Institute (IDIBGI), Girona, Spain*
[o] *Quantitative Imaging Biomarkers in Medicine (QUIBIM), Valencia, Spain*
[p] *Department of Physical Therapy, EUSES University School, Salt, Spain*
[q] *Center for Brain and Cognition, Universitat Pompeu Fabra, Barcelona, Spain*
[r] *ICREA Institut Catala de Recerca i Estudis Avançats, Barcelona, Spain*
[s] *Servei de Malalties Infeccioses, Fundació Irsicaixa, Hospital Universitari Germans Trias i Pujol, Badalona, Spain*
[t] *Universitat de Vic – Universitat Central de Catalunya (UVIC-UCC), Universitat Autònoma de Barcelona, Badalona, Spain*
[u] *Servei de Malalties Infeccioses, Fundacio de la Lluita contra la sida, Hospital Universitari Germans Trias i Pujol, Badalona, Spain*
[v] *Canon Medical Systems Europe, Zoetermeer, The Netherlands*
[w] *Olea Medical, La Ciotat, Marseille, France*
[x] *Department of Computer Science, Applied Mathematics and Statistics, University of Girona, Girona, Spain*
[y] *EURECAT, Technological Center of Catalonia, Barcelona, Spain*
[z] *Department of Endocrinology and Nutrition, Hospital Universitari Germans Trias i Pujol (UAB) Badalona, Barcelona, Spain*
[aa] *Division of Neurodegenerative Disorders, St. Boniface Hospital Albrechtsen Research Centre, Winnipeg, MB, Canada*
[bb] *Manitoba Learning and AI Research (MLAIR), University of Manitoba, Winnipeg, MB, Canada*
[cc] *Division of Image Processing, Department of Radiology, Leiden University Medical Center, Leiden, The Netherlands*
[dd] *Department of Neurology, University of Rochester, Rochester, NY, United States*
[ee] *Department of Radiology, University of Missouri, Columbia, MO, United States*
[ff] *Neuroradiology Section, Department of Radiology, Stanford University School of Medicine, Stanford, CA, United States*

[*] Corresponding authors at: Girona Biomedical Research Institute (IDIBGI), Hospital Universitari de Girona Dr Josep Trueta, Girona, Spain.
E-mail addresses: jpuigmd@gmail.com (J. Puig), rramos.girona.ics@gencat.cat (R. Ramos).

https://doi.org/10.1016/j.mad.2020.111257

Available online 11 May 2020

[gg] Department of Radiological Sciences, David Geffen School of Medicine, University of California, Los Angeles, CA, United States
[hh] Institut d'Assistència Sanitària, Salt, Spain

ARTICLE INFO

Keywords:
aging
biomarkers
radiomics
whole-body magnetic resonance imaging
population-based study
big data analyses

ABSTRACT

Biomarkers of aging are urgently needed to identify individuals at high risk of developing age-associated disease or disability. Growing evidence from population-based studies points to whole-body magnetic resonance imaging's (MRI) enormous potential for quantifying subclinical disease burden and for assessing changes that occur with aging in all organ systems. The Aging Imageomics Study aims to identify biomarkers of human aging by analyzing imaging, biopsychosocial, cardiovascular, metabolomic, lipidomic, and microbiome variables. This study recruited 1030 participants aged ≥50 years (mean 67, range 50–96 years) that underwent structural and functional MRI to evaluate the brain, large blood vessels, heart, abdominal organs, fat, spine, musculoskeletal system and ultrasonography to assess carotid intima-media thickness and plaques. Patients were notified of incidental findings detected by a certified radiologist when necessary. Extensive data were also collected on anthropometrics, demographics, health history, neuropsychology, employment, income, family status, exposure to air pollution and cardiovascular status. In addition, several types of samples were gathered to allow for microbiome, metabolomic and lipidomic profiling. Using big data techniques to analyze all the data points from biological phenotyping together with health records and lifestyle measures, we aim to cultivate a deeper understanding about various biological factors (and combinations thereof) that underlie healthy and unhealthy aging.

1. Introduction

Aging is a complex process characterized by a time-dependent decline in functional capacity and stress at different biological levels, associated with increased risk of morbidity and mortality (Clouston et al., 2013). The trajectories of aging in humans, vary widely due to genetic heterogeneity and environmental factors. The concept of biological age, unlike chronological age, takes these factors into account (Foo et al., 2019). Quantifiable age-related changes in body structure or function that could serve as measures of biological age, defined as the hypothetical underlying age of an organism, are termed biomarkers of aging (Simm et al., 2008). By definition, these biomarkers predict the trajectory of biological aging, thus the onset of age-related diseases. As age is a major risk factor for many degenerative diseases, these biomarkers could help identify individuals at high risk of developing age-associated diseases or disabilities (Simm et al., 2008; Baker and Sprott, 1988). Recently, different machine learning approaches have been proposed for the estimation of biological age, through a number of circulating and non-circulating biomarkers (Gialluisi et al., 2019). Identifying biomarkers with a significant influence on biological age and developing reliable models for its estimation is of fundamental importance for monitoring healthy aging, and could provide new tools to screen health status and the risk of clinical events in the general population.

Radiomics aims at developing imaging biomarkers by extracting information about quantitative features from different medical imaging modalities in population-based studies (Oakden-Rayner et al., 2017; Giger, 2018; Parekh and Jacobs, 2019). The choice of imaging modality depends primarily on the research focus, although other aspects such as reproducibility, availability, costs, general legal considerations, or risks are also important. Computed tomography, used to develop the first radiomic biomarkers in oncological studies, is limited by its use of ionizing radiation (Giger, 2018). Ultrasonography is inexpensive, convenient, and totally noninvasive, but has limited reproducibility. Nevertheless, ultrasonography measurement of carotid artery intima-media thickness is an established imaging biomarker for overall atherosclerotic burden (Simon et al., 2002). Magnetic resonance imaging (MRI) is being used increasingly in population-based studies because it provides high tissue contrast without using ionizing radiation (Völzke et al., 2011; Bamberg et al., 2015). MRI has generated substantial scientific knowledge about the human brain in population studies, such as the UK Biobank prospective epidemiological study (Miller et al., 2016), the Rotterdam Study (Verlinden et al., 2017), the Three-City Dijon Study (Tully et al., 2017) or the 1000BRAINS study (Caspers et al., 2014). MRI is also a routine clinical standard for examining the spine, cardiac structures and function, large blood vessels, and abdominal organs (Kuhl et al., 2008). Technological advances such as parallel acquisition technologies and continuous table feed have made it possible to examine the entire body in approximately 1 h. As a result, it is now feasible to incorporate whole-body MRI examinations into the design of population-based studies to acquire multiple datasets that, taken together, provide a holistic view of the human body (Kuhl et al., 2008). These studies can be used to characterize in an integrated manner the morphological and functional alterations of different organ systems, increasing our understanding of diseases in the community and providing knowledge about risk factors and outcomes.

Population-based cohort studies generally monitor participants through follow-up examinations. Two broad approaches are used to explore imaging datasets. Cross-sectional approaches correlate baseline image-based phenotypic features with non-imaging parameters, while longitudinal approaches correlate phenotypic features at different time points with clinical outcomes to determine their prognostic relevance. The inclusion of a large number of participants helps ensure adequate power to identify and verify associations [Coppola et al., 2019; European Society of Radiology (ESR), 2015]. Radiomics can reveal subtle microstructural alterations in tissues by analyzing variables such as volume, intensity, texture, and shape of neighboring voxels (Oakden-Rayner et al., 2017). The application of methods derived from the study of artificial intelligence, particularly machine learning can be used to determine which extracted image-based features and combinations of features are associated with different outcomes (Giger, 2018). Radiomics allows the development of image-based systems for risk stratification that promise to be useful for personalized medicine and prevention (Oakden-Rayner et al., 2017; Parekh and Jacobs, 2019). In other words, machine learning has enabled researchers to use multimodal MRI datasets to build predictive models of brain aging. These models assume a trajectory of brain aging that represents an individual's accumulation of changes that lead to alterations in structure and function of the brain and increased risk of cognitive decline and disease as well.

The multidisciplinary and multi-institutional Aging Imageomics Study set out to create a large repository of imaging datasets from advanced structural and functional whole-body MRI to enable the analysis of associations between imaging biomarkers and biopsychosocial parameters, cardiovascular indexes, metabolomics, lipidomics, microbiomics, frailty and other age-related variables. Analyzing what is

normal and abnormal during aging will allow to establish new reference ranges for variables related to aging. The ultimate goal is to combine data from whole-body imaging with data from other fields to develop a panel of biomarkers of biological aging that can identify individuals at high risk of developing age-associated diseases or disabilities. Here we report on the rationale, study design and logistics, technical background, and baseline characteristics of participants in the Aging Imageomics Study.

2. Methods

2.1. Aging imageomics consortium

A consortium of 14 partners was formed to enable an interdisciplinary approach to establishing biomarkers of biological aging in humans. The different partners have expertise in clinical radiology, epidemiology, primary care, bioengineering, neuroscience, physiology, endocrinology, cardiology, neurology, psychology, physiotherapy, cell biology and human genetics.

2.2. Study design, population and sample recruitment

The Aging Imageomics Study is an observational study that includes participants from two independent ongoing cohort studies with their own eligibility criteria of individuals residing in the province of Girona (Northeast Catalonia, Spain): the Maturity and Satisfactory Ageing in Girona study (MESGI50 study) (Corominas Barnadas et al., 2017) and the Improving interMediAte RisK management study (MARK study) (Martö et al., 2011). The MESGI50 study is a population-based cohort linked to the Survey of Health, Ageing and Retirement in Europe project (SHARE), which included a representative sample of the population of the province of Girona aged ≥50 years (Conde-Sala et al., 2017). The MARK study included a random sample of patients aged 35–74 with intermediate cardiovascular risk recruited in public primary care centers in the province of Girona (Martí et al., 2011). Members of both cohorts were contacted by telephone to be invited to participate in the Aging Imageomics Study. During this standardized telephone call, potential candidates were informed about the study and were encouraged to request more detailed information if they so desired. Subjects that agreed to participate were asked to choose a date and time to complete the enrollment procedures. To be eligible for the study, potential participants had to meet the following criteria: age ≥50 years, dwelling in the community (i.e. not institutionalized), no history of infection during the last 15 days, no contraindications for MRI (electronic cardiac implants, cochlear implants, incompatible prosthetic heart valves, incompatible vascular clips, metallic foreign bodies or claustrophobia), and consent to be informed of potential incidental findings.

2.3. Study procedures and ethical aspects

The Aging Imageomics Study protocol was approved by the ethics committee of Dr. Josep Trueta University Hospital. Data were collected between 14 November 2017 and 19 June 2019. Candidates were scheduled for two appointments. The first visit consisted of three parts. First, candidates were informed in detail about the study aims and characteristics. Second, candidates who provided informed written consent were assigned a personal identification code and then underwent whole body-MRI and carotid ultrasound studies. Third, participants were scheduled for the next examination (15 days later), and a research assistant provided them with a kit and detailed step-by-step instructions for collecting and transporting morning urine and stool samples to be presented on the day of the following visit. The second visit consisted of three parts. First, morning urine and stool samples were collected from participants, and blood samples were drawn between 8:00 a.m. and 10:00 a.m. After basic processing, specimens were transported to the IDIBGI's Biobank central laboratory by cold chain and were frozen at −80 °C for future use. Second, participants underwent an anthropometric examination, a clinical interview, and a cardiovascular examination by a trained nursing team. Third, participants completed standardized tests and questionnaires administered by the nursing team and trained psychology students to measure cognitive-, mood- and personality-related variables. Participants from the MARK study were also invited to further collaborate by using a device to measure ambient air pollution in the 2 weeks between visits. Table 1 lists the parameters assessed in each domain and the instruments used to measure them. At the end of the study, participants received a detailed report with the main findings of the MRI, carotid ultrasound, electrocardiogram and blood test.

Table 1
Domain, parameters and techniques for data acquisition.

Domain	Parameter	Instrument/technique
Anthropometry	Body height and weightWaist circumference	Scale and tape measure
Medical history	Self-reported diseasesMedication use	Ad hoc questionnaire
Cardiovascular system	Blood pressureAnkle-brachial indexHeart rate, PQ, QRS, QT, ST, QPulse wave velocityCarotid arteries characteristicsRetina vascular characteristics[a]	ElectrocardiogramUltrasoundRetinography
Cognitive function	MemoryProcessing speedAutomatic response inhibitionAttentionWorking memoryExecutive control and verbal ability	Memory Binding Test (Papp et al., 2015; Gramunt et al., 2016)Symbol Digit Modality Test (Smith, 1982)Color Word Stroop Test (Golden, 1978)Forward Digit Span Test (Wechsler, 1997)Backward Digit Span Test (Wechsler, 1997) Fluency Tasks (Lezak et al., 2012)
Personality	ExtraversionAgreeablenessContentiousnessNeuroticismOpenness	Big Five Inventory-10 (Rammstedt and John, 2007)
Emotion	Depressive symptomsManiac symptomsSuicidal ideation	Patient Health Questionnaire-9 (Kroenke and Spitzer, 2001) Mini International Neuropsychiatric Interview (Hypo)Manic Episode and Suicidality Modules (Sheehan et al., 1998)
Lifestyle	DietPhysical activity	PREDIMED Adherence to Mediterranean diet (Martínez-González et al., 2012)International physical activity questionnaire-SF (Craig et al., 2003)
Ambient air pollution[a]	Nitrogen dioxide levels	Passive diffusion tube
Basic biochemistry	Serum glucose, blood glycated hemoglobin, serum total, LDL and HDL cholesterol, fasting triglycerides, serum creatinine, sodium, potassium, calcium, phosphate, serum ferritin, serum thyroid stimulating hormone	Blood sample
Metabolomics, lipidomics, transcriptomics, and proteomics	Circulating metabolites, proteins, and mRNA from peripheral blood mononuclear cells	Blood and urine samples
Gut microbiota	Composition and metagenomics	Stool sample

[a] Only assessed in MARK sample participants.

2.4. Whole-body MRI acquisition protocol

MRI examinations were performed on a mobile 1.5 T scanner (Vantage Elan, Toshiba Medical Systems at the beginning of the study, now from Canon Medical Systems) using a head coil and two body coils to cover the body, with a maximum gradient amplitude of 35mT/m-1. Table 2 summarizes the MRI protocol. In brief, the acquisition protocol included (a) coronal T2-weighted half-fourier single-shot fast spin-echo (FSE) sequences and axial T1-weighted fast field echo of thoracoabdominal region from the neck to the upper thigh; (b) sagittal T2-weighted FSE of the whole spine; (c) short-axis 3D steady-state free precession sequences of the myocardium; (d) 2D phase-contrast magnetic resonance angiography (MRA) of the aortic arch; (e) fresh blood imaging non-contrast MRA of the abdominal aorta and iliac segments; (f) axial T1-weighted water fat suppression (Dixon's technique) from the liver to the symphysis pubis; (g) axial and coronal quantitative T2* mapping using gradient multiecho at 6 echo times; and (h) diffusion tensor imaging (DTI) using spin echo echo-planar imaging (SE-EPI), resting-state functional MRI (rs-fMRI) using gradient echo EPI, R2* mapping using multiecho gradient echo sequence, high resolution 3D T1-weighted magnetization prepared rapid acquisition gradient echo (MPRAGE) and 2D T2-weighted fluid attenuated inversion recovery (FLAIR) sequences of the brain. The complete MRI protocol took about 50 min. Fig. 1 is a graphic representation of each of the acquisitions; Fig. 2 shows the imaging variables collected in each body region.

2.5. Quality control of the MRI examinations

The four medical imaging technologists involved in MRI acquisition completed a one-month training program on the imaging platform provided by the vendor and further training. That additional training included the observation and hands-on whole-body MRI acquisition in different MRI units at several university institutions before starting the project. These technologists visually checked the quality of the images obtained during the acquisition process. A dedicated MRI physicist and a radiologist (13 years' experience) also reviewed subsets of the images to ensure acquisition standards were met. The MRI physicist supervised regular MR phantom measurements for quality control.

2.6. Carotid ultrasound study

A radiologist (13 years' experience) performed all carotid ultrasound examinations on a Siemens Acuson S2000 system (Mochida Siemens Medical System; Tokyo, Japan) system with a 7.5 mHz linear array transducer, measuring carotid stenosis percentage on B-mode (common carotid artery and internal carotid artery). After capturing a transverse scan of the most stenotic segment, the original diameter and residual diameter were measured using electronic calipers. The residual diameter was defined as the shortest diameter of the residual lumen at the most stenotic carotid segment. On the other hand, the original diameter was defined as the measured diameter from the outer media to the outer media of the diseased artery on the same plane and at same direction with the residual diameter. This value was calculated using the following equation: Carotid stenosis percentage = (1 − [residual diameter/original diameter]) × 100, as previously described (Lee et al., 2011; Lemne et al., 1995; Wendelhag et al., 1991). The carotid intima–media thickness and plaques will be measured according to the Mannheim Consensus (Touboul et al., 2012).

2.7. Data collection and storage

Two databases were used. The participant's name and study identification code were inputted with individual passwords in an encrypted database. All data from questionnaires and medical devices were entered in another anonymous electronic database using the personal study identification code. A data manager checked the entries for completeness and plausibility and amended incomplete or implausible data when possible. Further data from biological samples and MRI postprocessing were linked through the personal study identification code. Encrypted backups of both databases were periodically stored on two external hard disks kept at different sites.

2.8. Ongoing data analysis

To extract biomarkers of aging and construct a healthy aging model, correlation analyses will be used to identify relationships between different measurements and machine learning methods will be used to estimate biological age from the imaging data and other measurements. Neural networks and decision/regression trees will be applied to find more local relationships within the data. Besides, dimensionality reduction techniques (e.g. principal component analysis) are needed to reduce the number of measurements required and variance in the predictions. Machine learning tools make it possible to combine diverse predictors to generate models with lower variance. Data visualization techniques and interactive methods such as visual clustering models might further help uncover unexpected relationships and reduce

Table 2
Magnetic resonance imaging protocol.

Anatomic coverage	Sequence	Imaging parameters[a] (TR; TE; FA; VS, FOV)
Thoracoabdominal[b]	T2-weighed half-fourier single-shot FSE	3850; 78; 90; 0.6 × 0.6 × 7.5; 400
	3D T1-weighed FFE	4.4; 1.9; 13; 0.9 × 0.9 × 6.8; 490
Brain	2D FLAIR	6160; 105; 90; 0.5 × 0.5 × 5; 230; inversion time, 2100 ms
	Resting-state BOLD (gradient echo EPI)	2500; 40; 83; 3.5 × 3.5 × 5; 230
	Diffusion tensor imaging (spin echo EPI)	5900; 96; 90; 1 × 1×3; 230
	R2* mapping (multiecho gradient echo)	750; 4.6 Δ4.6; 15; 1 × 1 × 6; 230
	3D T1-weighted (MPRAGE)	8; 4.5; 15; 1.2 × 1.2×2.5; 230; inversion time, 620 ms, recovery time, 500 ms
Heart	Cine SSFP short axis	4.2; 2.1; 41; 1.7 × 1.7 × 12; 360
Aortic flow	2D phase-contrast MRA	10.5; 5; 20; 0.8 × 0.8 × 6; 380
Abdominal aorta and iliac segments	3D non-contrast MRA (fresh blood imaging)	2244; 80; 90;0.6 × 0.6 × 4; 450
Abdomen	3D T1-weighted WFS (Dixon's method)	8.9; 1.3 Δ2.3; 12; 1.4 × 1.4 × 8.2; 450
Abdomen	2D gradient multiecho (6 echo time) (Quantitative T2* mapping)	16.2; 2.3Δ2.3; 10; 1.4 × 1.4 × 10; 420
Whole spine	T2-weighted 2D FSE	4650; 120; 90; 0.5 × 0.5 × 4; 400 (for two steps)

BOLD, blood oxygen level-dependent; EPI, echo-planar imaging; FLAIR, fluid attenuated inversion recovery; FFE, fast field echo; FSE, fast spin echo; MPRAGE, magnetization prepared rapid gradient echo; MRA, magnetic resonance imaging; SSFP, single short-axis 3D cine steady-state free precession; WFS, water fat suppression.

[a] TR, repetition time (ms); TE, echo time (ms); FA, flip angle (degree); VS, voxel size (mm^3); FOV, field of view (mm^2).

[b] From the neck to the upper thigh.

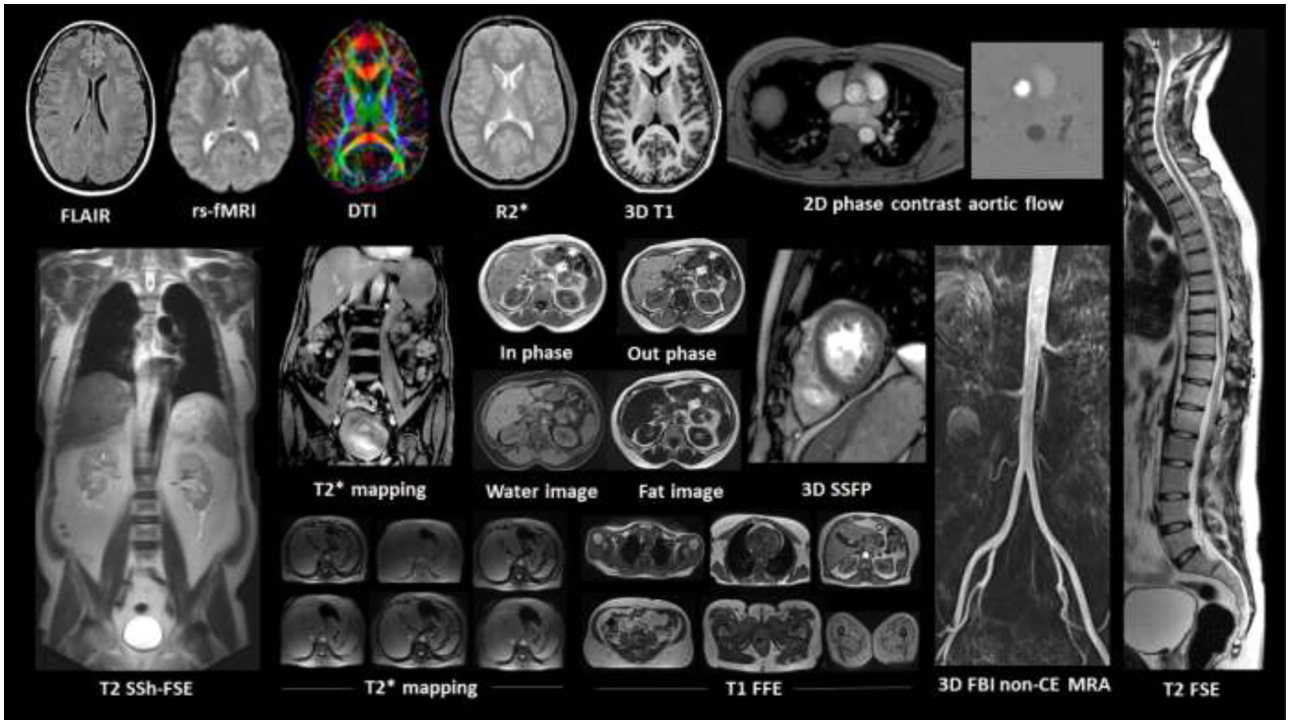

Fig. 1. Magnetic resonance imaging acquisition protocol. DTI, diffusion tensor imaging; FLAIR, fluid attenuation inversion recovery; rsfMRI, resting-state functional magnetic resonance imaging; SSFP, steady-state free precession; SSh-FSE: single-shot fast spin echo; TSE, turbo spin echo.

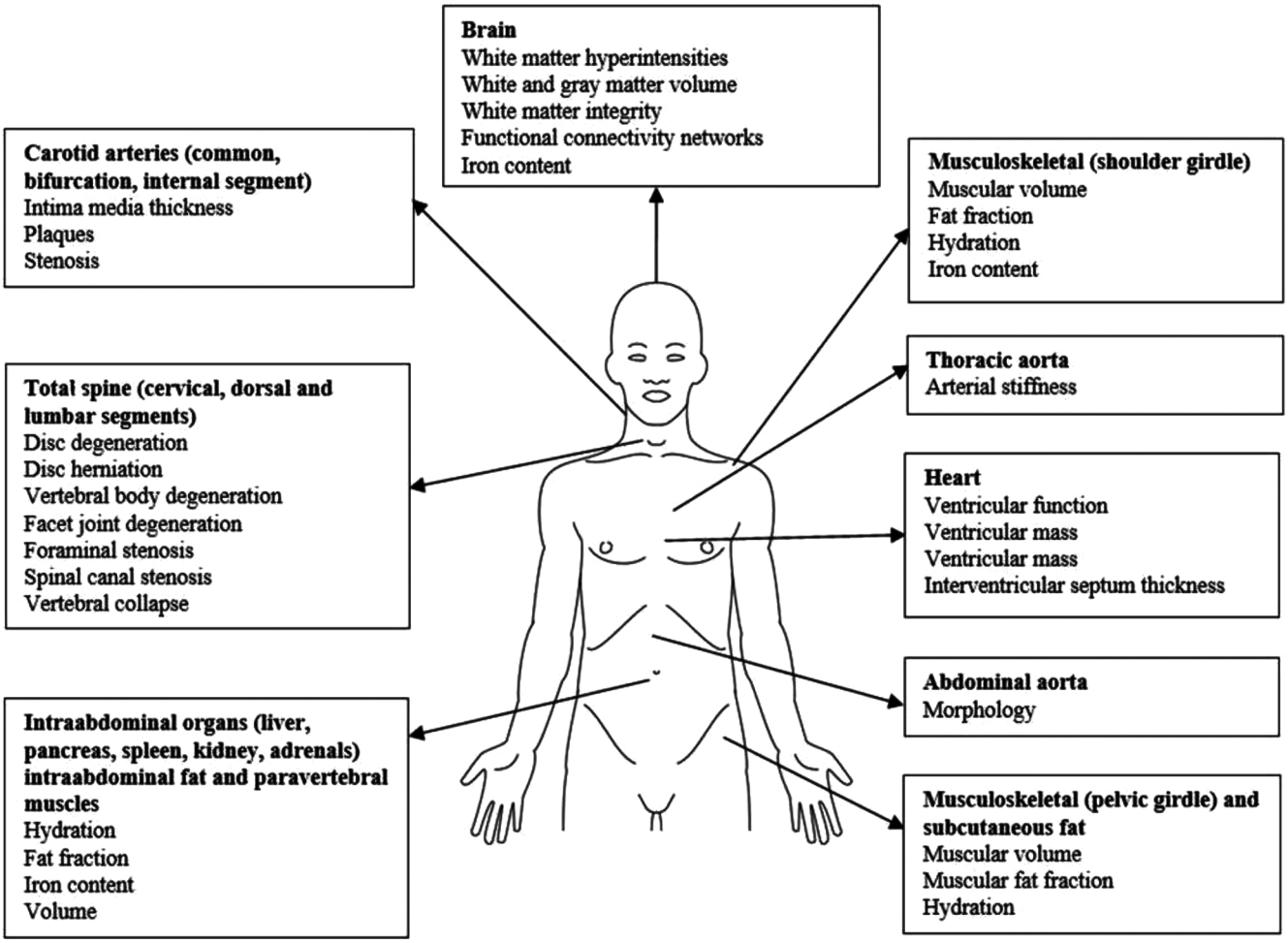

Fig. 2. Major phenotypic features analyzed in the Aging Imageomics Study.

variance in the models by improving the characterization of subgroups. One end-product will be the creation of a structural and functional imaging atlas to model the aging of organs.

2.9. Incidental findings

Potentially clinically relevant abnormalities discovered on examinations done for unrelated purposes are referred to as incidental findings. Two certified radiologists with 25 and 13 years' experience reviewed all whole-body MRI and carotid ultrasound images for incidental findings. Following the approach used in the German National Cohort (Schlett et al., 2016), incidental findings were classified as "notification urgently required", "notification required" and "notification not required", based on the likelihood of false-positive findings, clinical consequences of the finding and potential negative consequences for the participant if unaware of the finding.

2.10. Statistical analysis

For participants' demographic and health characteristics, qualitative variables are expressed as absolute and relative frequencies and quantitative variables as measures of central tendency and dispersion. For bivariate comparisons of these variables between cohorts, chi-square tests, Mann–Whitney *U* tests or Kruskall–Wallis tests are used. To assess the effect size for differences between proportions, Cramer's *V* was applied, the value of which depends on the degrees of freedom (df = 1; small [0.10], medium [0.30], large [0.50]; df = 2; small [≤0.07], medium [0.21], large [≥0.35]; df3 = small [≤0.06], medium [0.17], large [≥0.29]). The effect size for differences between two means was assessed by Cohen's *d* (small = 0.2; medium = 0.5; large = 0.8) (Fritz et al., 2012). Ninety-five percent confidence intervals (95 % CIs) for incidental finding prevalence rates were calculated assuming a Poisson distribution. For all analyses, we used STATA 12 SE (STATA Corp., College Station, TX, USA) and a two-tailed alpha level for statistical significance corrected for multiple comparison using the Bonferroni adjustment ($p < 0.001$).

3. Results

The Aging Imageomics Study finished the recruitment of participants by June 2019. All participants in the MARK and MESGI studies ($n = 2181$) were considered potential candidates; 1741 met the inclusion criteria. Fig. 3 is a flowchart showing the process of inclusion in the study. The final study population consisted of 1030 participants (mean age, 67.1 ± 7.3 years; range, 50–98 years; 54.1 % male); 567 (55.0 %) were recruited from the MARK study cohort (57.1 % of all candidates in

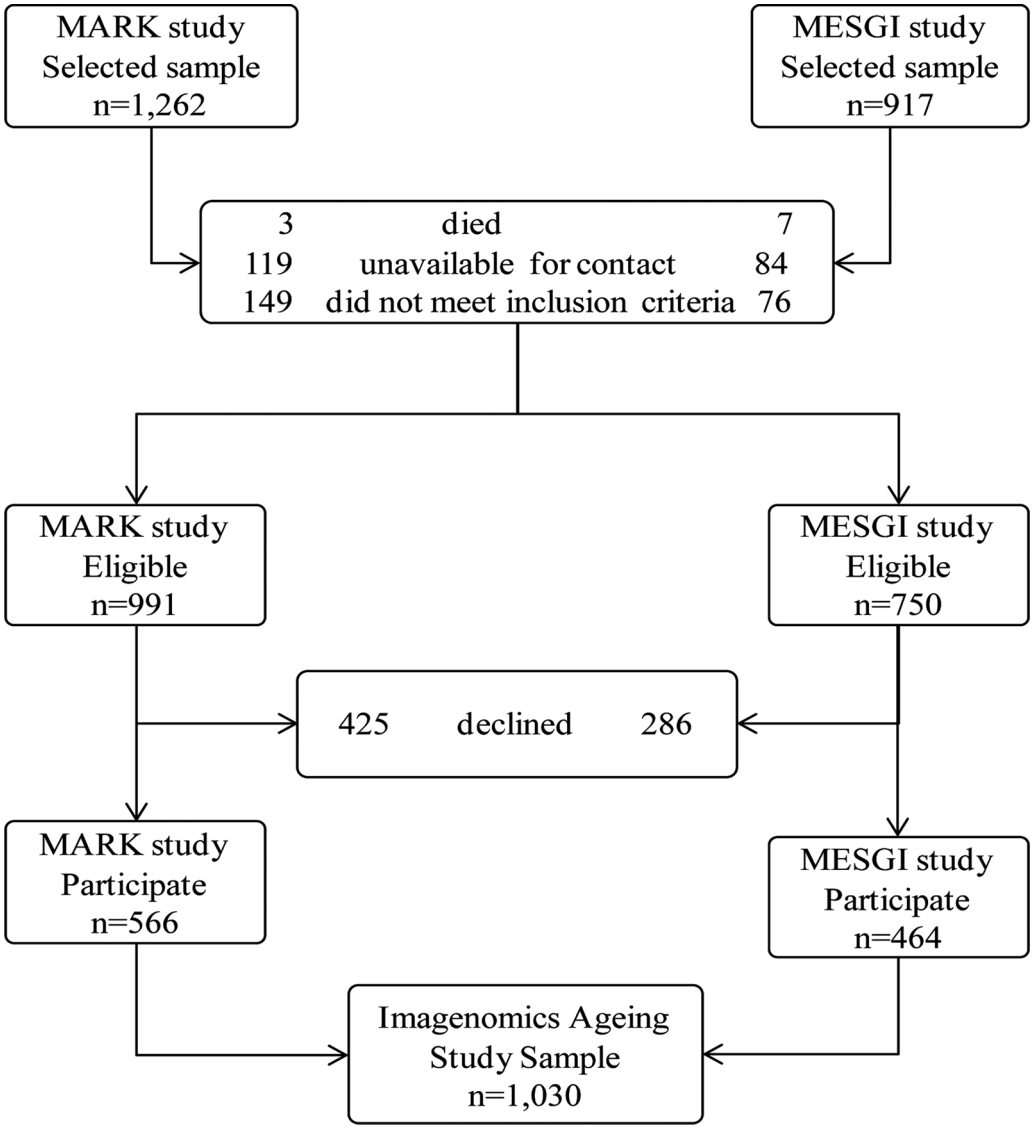

Fig. 3. The Aging Imageomics Study participation flowchart.

that study) and 463 (45.0 %) from the MESGI study cohort (61.8 % of all candidates from that study). Education level was classified as low in 57.3 %, intermediate in 30.7 % and high in 12.0 %; 71.3 % were retired, 23.1 % employed and 5.6 % unemployed or on sick leave. These variables differed slightly between women and men: educational level was slightly higher in men, and a slightly higher proportion of women were unemployed or sick (Table 3).

Table 4 summarizes participants' anthropometric characteristics, vascular system health status, medical history, basic biochemistry results and carotid ultrasound examination results, stratified by gender. As expected, anthropometric characteristics (weight, height, waist circumference, heart rate and blood pressure) differed between women and men (p values < 0.001 and moderate to large effect size). A greater percentage of women had a personal history of depressive episodes (42.3 % vs. 18 % in men). Differences with moderate effect size were observed in some biochemistry results (HDL cholesterol, creatinine, sodium, potassium and serum ferritin). Severe carotid stenosis was more common in men (13.1 % vs. 6.3 % in women).

Table 5 reports lifestyle indicators (e.g. Mediterranean diet adherence, physical activity pattern), personality traits, affective status and neuropsychological examination results, stratified by gender. A greater proportion of women had the personality trait "neuroticism" and depressive symptoms (p values < 0.001 and moderate effect size). Women outperformed men in memory-related neuropsychological tasks (p values < 0.001 and moderate effect size).

Supplemental Tables S1–S3 report the demographic, social and clinical characteristics of the participants, stratified by the cohort of origin (MARK vs. MESGI). As expected, participants from the two cohorts differed in some clinical and demographic characteristics. Although MARK study participants were recruited from primary care centers on a random basis, only those with intermediate cardiovascular risk were candidates; consequently, characteristics related to cardiovascular health status differed between the two cohorts. Compared to participants recruited from the MESGI cohort, those recruited from the MARK study had higher weight (77.8 kg vs. 73.1 kg), lower HDL cholesterol (49.3 mg/dL vs. 57.6 mg/dL), and higher serum glucose (116.4 mg/dL vs. 104.8 mg/dL) and blood glycated hemoglobin (6.1 % vs. 5.7 %) (p values < 0.001 and moderate effect size). Lifestyle and personality characteristics in participants from the two cohorts were similar, but participants coming from the MESGI study outperformed those coming from the MARK study in all the neuropsychological tasks (p values < 0.001 and moderate effect size).

The prevalence of incidental findings on whole-body MRI requiring notification was 4.44 % (96 % CI = 3.28–5.91); the most frequent incidental findings requiring notification were located in the brain (1.35 %), followed by the abdomen (1.16 %), spine (0.77 %), thorax (0.58 %) and genitourinary regions (0.58 %). A more detailed classification of incidental findings is provided in Table S4.

4. Discussion

The Aging Imageomics Study used multiple imaging modalities to acquire data about the brain, spine, abdomen, heart, musculoskeletal system and large blood vessels with sufficient statistical power for reliable assessment of associations between imaging phenotype measures and a wide range of parameters related to aging. By analyzing these associations, we aim to develop a panel of combined biomarkers of aging that will be useful for characterizing biological age and identifying individuals at high risk of developing age-associated diseases or disabilities. Participants were drawn from two population-based cohorts, one representative of the general population and another comprising individuals with intermediate cardiovascular risk. Comparing these two cohorts will help in identifying and validating potential biomarkers of aging.

4.1. "Biomarkers of aging" and "biological age score"

The rate of aging, measured as the decline of functional capacity and stress resistance, differs significantly among individuals, thus giving rise to differences between biological and chronological age in some of them (Foo et al., 2019). Classically, the rate of aging of a given population has been quantified by calculating the slope of the mortality curve. However, in this approach, it is only possible to determine individuals' biological age at a given point in their lifetime retrospectively (i.e. after they have died), thus precluding reliable assessment of aging, risk prediction of the onset of morbidity and residual lifetime for a given living individual. One strategy to overcome this problem is to identify age-related changes in the body (biomarkers of aging) that could serve as surrogate measures of biological age and predict the onset of age-related diseases and/or residual lifetime more accurately than chronological age (Simm et al., 2008; Gialluisi et al., 2019).

The American Federation for Aging Research has proposed that biomarkers of aging should fulfill the following criteria (Johnson, 2006): (1) they must predict the rate of aging, signaling an individuals' exact point in their total lifespan better than chronological age; (2) rather than focusing on the effects of disease, they must focus on basic processes underlying the process of aging; (3) they must be noninvasive (e.g. imaging or blood tests) to allow repeated testing; (4) they must work in laboratory animals as well as in humans so that they can be tested in animals before being validated in humans.

In the last years, various biomarkers of aging have been proposed, but all have shown considerable variability in cross-sectional studies (Foo et al., 2019; Simm et al., 2008; Baker and Sprott, 1988; Gialluisi et al., 2019; Johnson, 2006; Bai, 2018). No single measurement has proven capable of accurately determining biological age. However, the process of aging is complex, involving multiple causes and multiple systems, so a panel of biomarkers reflecting this complexity is likely to measure biological age better than any single marker alone. Thus, the Aging Imageomics Study aims to devise a "biological aging score" by using multivariate analysis and modern Mmachine Llearning techniques to optimize the weighting of predictors from imaging (radiomics) and other tests (other omics). Recently, machine learning analysis of neuroimaging data have been applied to predict chronological age in healthy people (Cole and Franke, 2017; Cole et al., 2017). These models have been used to generate a biological age from neuroimaging data, a "brain-predicted age". If an individual's brain-predicted age is greater

Table 3
Demographic and social characteristics.

	Female (n = 473)	Male (n = 557)	p Value (effect size)
Age, mean (SD)	66.5 (7.7)	67.5 (7.0)	0.035 (< 0.1[a])
Age groups			0.152 (0.06[b])
50 − 64	209 (44.2)	210 (37.7)	
65 − 74	201 (42.5)	260 (46.7)	
75 +	63 (13.3)	87 (15.6)	
Education level completed			< 0.001 (0.14[b])
None	24 (5.2)	8 (1.5)	
Primary (ISCED 1)	248 (53.4)	295 (54.5)	
Secondary (ISCED 2)	55 (11.9)	93 (17.2)	
Professional (ISCED 3 − 4)	87 (18.8)	74 (13.7)	
University (ISCED 5 − 8)	50 (10.8)	71 (13.1)	
Working status			0.021 (0.08[b])
Retired	314 (67.8)	403 (74.2)	
Employed	114 (24.6)	118 (21.7)	
Other (unemployed/sick)	35 (7.6)	22 (4.1)	

ISCED, International Standard Classification of Education, 1997 levels.
[a] Cohen's d.
[b] Cramer's V.

Table 4
Physical anthropometrics and health characteristics.

	Female (n = 473)	Male (n = 557)	p Value (effect size)
Weight (kg), mean (SD)	69.5 (14.0)	81.2 (11.8)	< 0.001 (0.90[a])
Height (cm), mean (SD)	158 (6.6)	170 (6.8)	< 0.001 (1.7[a])
Waist circumference (cm), mean (SD)	95.6 (13.0)	101.8 (10.2)	< 0.001 (0.51[a])
Number of medications, mean (SD)	2.6 (2.3)	2.2 (1.9)	0.066 (0.18[a])
Heart rate (bpm), mean (SD)	67.2 (11.8)	63.6 (12.7)	< 0.001 (0.29[a])
Systolic arterial pressure (mmHg), mean (SD)	138.2 (19.5)	140.4 (19.3)	0.070 (0.11[a])
Diastolic arterial pressure (mmHg), mean (SD)	82.9 (11.1)	84.7 (10.4)	< 0.001 (0.16[a])
Ankle–brachial index test, n (%)			
Left, normal 1.0–1.4	422 (92.5)	510 (94.8)	0.114 (0.04[b])
Right, normal 1.0–1.4	423 (92.8)	504 (94.2)	0.227 (0.06[b])
Personal medical history, n (%)			
Hypertension	193 (41.6)	278 (51.2)	0.002 (0.09[b])
Diabetes mellitus	94 (20.3)	119 (21.9)	0.533 (0.02[b])
Dyslipidemia	127 (27.4)	166 (30.6)	0.265 (0.03[b])
Congestive heart failure	4 (0.9)	10 (1.8)	0.192 (0.04[b])
Atrial fibrillation	9 (2.0)	11 (2.0)	0.934 (< 0.01[b])
Chronic kidney disease	20 (4.3)	26 (4.9)	0.682 (0.01[b])
Chronic obstructive pulmonary disease	5 (1.1)	10 (1.9)	0.314 (0.03[b])
Depressive episode	192 (42.3)	94 (18.0)	< 0.001 (0.26[b])
HDL cholesterol (mg/dL), mean (SD)	58.2 (16.5)	48.6 (13.2)	< 0.001 (0.64[a])
LDL cholesterol (mg/dL), mean (SD)	122.0 (30.5)	115.9 (31.4)	0.003 (0.19[a])
Fasting triglycerides (mg/dL), mean (SD)	118.6 (63.0)	125.1 (81.2)	0.275 (< 0.01[a])
Serum glucose (mg/dL), mean (SD)	108.5 (32.1)	113.7 (25.8)	< 0.001 (0.17[a])
Fasting plasma insulin (mg/dL), mean (SD)	9.7 (6.7)	11.2 (8.4)	< 0.001 (0.19[a])
Blood glycated hemoglobin (%), mean (SD)	5.9 (0.9)	5.9 (0.8)	0.697 (< 0.01[a])
Serum creatinine (mg/dL), mean (SD)	0.73 (0.16)	0.96 (0.20)	< 0.001 (1.26[a])
Sodium (mEq/L), mean (SD)	142.1 (2.1)	141.5 (2.0)	< 0.001 (0.29[a])
Potassium (mEq/L), mean (SD)	4.5 (0.4)	4.7 (0.4)	< 0.001 (0.50[a])
Calcium (mg/dL), mean (SD)	9.5 (0.4)	9.4 (0.4)	< 0.001 (< 0.01[a])
Phosphate (mg/dL), mean (SD)	3.6 (0.4)	3.2 (0.4)	< 0.001 (1.0[a])
Serum ferritin (ng/dL), mean (SD)	102.5 (80.7)	205.1 (171.2)	< 0.001 (0.76[a])
Thyroid stimulating hormone (mUI/L), mean (SD)	3.0 (5.7)	2.4 (2.4)	< 0.001 (0.13[a])
Carotid ultrasound examination, n (%)			< 0.001 (0.18[b])
Normal	204 (45.6)	154 (29.7)	
Non-severe stenosis (< 70 %)	215 (48.1)	297 (57.2)	
Severe stenosis (≥70 %)	28 (6.3)	68 (13.1)	

[a] Cohen's d.
[b] Cramer's V.

than their chronological age, this indicates that their brain structure more closely resembles a healthy person who is older than they are (Cole and Franke, 2017). The assumption is that greater discrepancies between brain-predicted age and chronological age reflect poorer brain health, for a given age. Deviations from healthy brain aging have been associated with cognitive impairment and disease. However, key to validating "brain-predicted age" biomarker is to relate it to other measures of aging, such as cognitive or physiological assessments (Cole et al., 2019). In a recent study (Cole et al., 2018), using measures of brain volume general population, narrow age-range (approximately 73 years old) cohort, brain-predicted age was calculated for 669 people. Cole et al. (2018) demonstrated that having a brain-predicted age indicative of an older-appearing brain was associated with weaker grip strength, poorer lung function, slower walking speed, lower fluid intelligence, higher allostatic load and increased mortality risk. This suggests that measures of age-associated brain volume are sensitive to the same underlying factors that cause physiological changes during aging. Lastly, an automated machine learning data-driven approach has been proposed to predict brain age from cortical measures (Dafflon et al., 2019). Preliminary results suggest that the accuracy of these models might be better than recent brain age models.

Although telomere length is one of the most plausible biological age predictors, it seems to be less appropriate than brain-predicted age, either at predicting chronological age or health outcomes (Jylhävä et al., 2017). The composite biomarker is not validated enough but has the potential to be a stronger predictor than telomeres, as is the Metabolic Age Score (Jylhävä et al., 2017; Hertel et al., 2016). Other biological age predictors may prove to be useful, but would require further independent validation (Srivastava, 2019).

4.2. Precision medicine, radiomics and aging phenotyping

Artificial intelligence techniques are enabling progress toward precision medicine that takes differences among individuals into account to improve the prevention and treatment of disease (Hamet and Tremblay, 2017). Precision medicine depends on the availability of knowledge that allows differentiation among individuals. Determining a given individual's state of health requires combining data about many factors beyond chronological age, such as genetic, microbiomic, clinical, psychosocial and lifestyle-related characteristics (Williams et al., 2018). In aging, precision medicine should aim to classify individuals into subpopulations with different burdens of subclinical disease or susceptibilities to a disease according to observable phenotypes that reflect both genomic variation and accumulated lifestyle and environmental exposures that impact biological function (Snyderman, 2012). Genomics has been a useful approach for finding useful biomarkers for precision medicine, but non-genetic factors account for 70 %–90 % of the phenotypic variation in chronic and age-related diseases (Franceschi et al., 2018). Thus, effective and efficient approaches incorporating data from noninvasive medical tests are necessary to better define phenotypes of health and aging. National and international efforts such as the Aging Imageomics Study seek to collect a wide array of

Table 5
Lifestyle, personality characteristics, emotional status and cognitive function.

	Female (n = 473)	Male (n = 557)	p Value (effect size)
Adherence to Mediterranean diet, n (%)			0.663 (0.02[a])
Low	33 (7.6 %)	46 (8.8)	
Moderate	256 (59.0)	314 (60.0)	
High	145 (33.4)	163 (31.2)	
Physical activity, n (%)			< 0.001 (0.13[a])
Low (< 600 MET-minutes/week)	43 (9.9)	36 (6.9)	
Moderate (600 − 2999 MET-minutes/week)	213 (49.0)	200 (38.3)	
High (≥ 3000 MET-minutes/week)	179 (41.1)	286 (54.8)	
Personality traits			
Extraversion, mean (SD)	6.8 (1.7)	6.7 (1.8)	0.305 (0.05[b])
Agreeableness, mean (SD)	7.0 (1.6)	6.9 (1.6)	0.476 (0.06[b])
Conscientiousness, mean (SD)	7.6 (1.7)	7.6 (1.8)	0.870 (< 0.01[b])
Neuroticism, mean (SD)	5.9 (1.8)	5.4 (1.7)	< 0.001 (0.28[b])
Openness, mean (SD)	6.7 (1.8)	6.6 (1.8)	0.661 (0.05[b])
Patient health questionnaire-9, mean (SD)	5.2 (4.6)	3.0 (3.3)	< 0.001 (0.54[b])
Cognitive function, mean (SD)			
MBT – total paired recall	21.7 (5.1)	20.4 (5.0)	< 0.001 (0.25[b])
MBT – total free recall	12.5 (4.9)	10.7 (4.8)	< 0.001 (0.37[b])
MBT – total delayed paired recall	21.2 (5.3)	19.3 (5.2)	< 0.001 (0.36[b])
MBT – total delayed free recall	12.4 (5.1)	10.8 (4.8)	< 0.001 (0.32[b])
Forward digit span test	7.5 (2.9)	7.9 (2.1)	0.003 (0.15[b])
Backward digit span test	4.1 (1.8)	4.7 (1.9)	0.017 (0.32[b])
Symbol digit modality test	46.7 (19.7)	47.1 (17.2)	0.493 (0.02[b])
Letter fluency task	12.1 (4.8)	12.2 (4.8)	0.984 (< 0.01[b])
Category fluency task	16.5 (5.2)	16.7 (5.0)	0.190 (0.03[b])
Stroop test – words	81.7 (19.9)	82.2 (18.6)	0.802 (0.02[b])
Stroop test – colors	58.9 (13.9)	56.2 (14.1)	0.002 (0.19[b])
Stroop test – words/colors	32.6 (11.2)	33.1 (12.3)	0.750 (0.26[b])
Stroop test – interference	−1.4 (9.3)	−0.03 (10.6)	0.040 (0.13[b])

[a] Cramer's V.
[b] Cohen's d.

individual data, including genomic, proteomic, microbiomic and/or imaging data.

Computer analysis of medical images is a promising source of information for precision medicine initiatives. Medical images contain dense, objective data that can be useful for phenotyping (Larue et al., 2017). Radiomics uses high-throughput computational techniques to analyze data from medical images, considering both "traditional" image analysis with human-defined image features and "deep learning", where computer algorithms automatically discover features that are useful for specific purposes through a process of optimization incorporating data from different levels (Kumar et al., 2012). Deep learning methods can potentially discover aging biomarkers without any human input, conceivably generating truly unexpected discoveries. Including more variables and more data is likely to better reflect underlying aging process and improve phenotyping (Engchuan et al., 2019; Caballero et al., 2017; Mount et al., 2016). Although radiomics-based phenotyping has unmatched potential, its inherent complexity and lack of firmly established standards can lead to methodological variability and consequent risk of irreproducible results. It can be difficult to incorporate multiparametric data. Moreover, the large number of features extracted increases the risk of overfitting the data, so one of the first steps in analyzing radiomics data is to reduce the number of dimensions of the parameters to allow more robust and reliable analyses of a given dataset. One strategy is to select features based on technical qualities such as reproducibility across different settings or readers. Although the research community agrees that radiomics techniques need to be validated to ensure the repeatability, reproducibility, robustness and accuracy of the biomarkers derived from them as recommended by the Quantitative Imaging Biomarkers Alliance, there is no consensus about the best approach to data dimensionality reduction (Obuchowski et al., 2016, 2015, 2019).

4.3. MRI and radiomics

Extracting radiomics features from multimodal MRI sequences promises to advance aging phenotyping. MRI enables examiner-independent visualization of morphologic and functional processes without the need for contrast agents or ionizing radiation, providing simultaneous coverage of major organ systems in a single, whole-body examination requiring less than 1 h (Zenge et al., 2005; Bezerra et al., 2019). These examinations enable comprehensive quantitative assessment of adipose tissue distribution, brain and heart morphology and function, thoracic and abdominal organs, major blood vessels and the musculoskeletal system with high sensitivity and specificity (Kuhl et al., 2008). The capability of detecting subclinical disease and normal variants of the different organ systems have enormous potential for phenotyping in population-based studies assessing asymptomatic individuals. Although gadolinium-based contrast agents could provide additional useful information in MRI studies, their use requires the assessment of kidney function and the placement of an intravenous line and also involves a very small risk of allergic reactions (Schieda et al., 2018; Czeyda-Pommersheim et al., 2017). For these reasons, we decided not to use them in this population-based study.

4.4. Whole-body in MRI population-based studies

In recent years, several population-based studies have identified novel imaging biomarkers of preclinical disease (Hofman et al., 2011; Splansky et al., 2007; Bild et al., 2002; Schmermund et al., 2002; The ARIC Investigators, 1989). Examples include computed tomography assessment of coronary calcification (Detrano et al., 2008; Erbel et al., 2010), MRI assessment of left ventricular function/fibrosis or hepatic steatosis (Chuang et al., 2012; Kühn et al., 2012), and ultrasound

assessment of carotid intima–media thickness (Hegenscheid et al., 2009). However, imaging in population-based studies requires a robust and convenient modality that can be applied in many consecutive participants without major deviations, interruptions or cancellations; it also needs to be extremely safe, because the large sample size means that even very rare adverse events may occur. Moreover, the selected imaging modality should not alter the natural development of disease or potentially increase the risk for study endpoints (e.g. exposure to radiation from computed tomography and development of cancer). Finally, it should cover a large area of the body and provide high spatial resolution to assess subtle pathologic changes indicative of subclinical disease in different organ systems. Whole-body MRI meets these criteria, although contraindications may limit the target population and introduce a selection bias.

In addition to Aging Imageomics Study, various population-based studies are currently using whole-body MRI. In Germany, the German National Cohort aims to recruit 30,000 participants (Bamberg et al., 2015), the Study of Health in Pomerania (SHIP) has 3400 participants (Hegenscheid et al., 2009), and the Cooperative Health Research in the Augsburg Region (Kooperative Gesundheitsforschung in der Region Augsburg) (KORA) has 18,000 participants (Hetterich et al., 2016). In the United Kingdom, an extension of the UK Biobank (Miller et al., 2016; Petersen et al., 2013) study was funded in 2016 to collect imaging data (MRI of the brain, heart and body, low-dose X-ray bone and joint scans and ultrasound of the carotid arteries) from 100,000 subjects from the existing cohort by 2022. In the Aging Imageomics Study, integrating data from imaging with data from various sources is expected to provide unique insights into the biological mechanisms of aging. For example, structural and functional brain connectivity and cognitive performance may be linked to factors related to the microbiome, heart structure and function, carotid plaques, or body fat. The Aging Imageomics Study's multimodality imaging and multidisciplinary approach might identify intertwining risk factors.

4.5. Incidental findings

Whole-body MRI is bound to detect incidental findings in any large cohort of asymptomatic, supposedly healthy volunteers. The significance of these findings can be difficult to discern and might be considerably different from that of similar abnormalities in symptomatic individuals. How to deal with incidental findings is an ethical and practical quandary, because although these findings may identify potentially treatable disease, they may also represent false-positive findings or conditions that might never cause problems in the individual's life, in which case any further workup or follow-up would cause unnecessary psychological and/or physical suffering (Kwee and Kwee, 2019; Hegedüs et al., 2019).

4.6. Usefulness of biomarkers of biological aging

Since the ultimate goal of population-based studies is to learn about the overall health of the population and how to improve it, the data collected in the Aging Imageomics Study will be available to the national and international scientific community. Furthermore, the study has been designed to enable pooling of MRI data with other European and non-European cohorts to make it possible to identify small observable variations between subgroups of participants. Increased life expectancy of human beings worldwide will probably be accompanied by an increase in the prevalence of age-related diseases, thus increasing the need for effective strategies to prevent these conditions and diagnose them early. If biomarkers of aging identified individuals with high risk of developing age-associated disease or disability, detecting a faster-than-normal trajectory of aging, additional diagnostic and prophylactic measures (e.g. changes in lifestyle) might be indicated and early-stage treatment of age-related disease could be offered when available. Biomarkers would also be useful for assessing the efficacy of interventions to decrease the risk of age-associated disease in the entire population. Therefore, the results of these projects can be useful for public health officials, researchers, healthcare providers and health-related industry, as well as for the general public. Health managers need solid tools to assess overall community health so they can apply health plans and direct financial resources. Imaging biomarkers based on whole-body MRI and related data can be useful for monitoring the effects of future primary prevention strategies and for stratifying the population for specific health promotion and primary prevention programs.

To develop a validated panel of biomarkers that can predict the health span rather than only focus on mortality and lifespan is a challenging task for the research community. This could include marker combinations, such as a panel of physiologic, whole-body imaging, genomic and blood-based determinants, that predict the years a person would spend being free from frailty before death. Ideally, this panel of markers would be a useful indicator both in mid- and late-life (Jylhävä et al., 2017). For this, we will need to have access to longitudinal data, and will work at addressing the vast variability among participants, and potential for confounding.

5. Conclusions

In summary, the population-based Aging Imageomics Study represents an opportunity to better understand the physiological processes associated with aging in the human body. This data might be useful to quantify biological aging using as biomarkers tissue changes, as measured by MRI and US, and metabolic changes and relating them to clinical outcomes. This project will allow us to determine a range of normal values for each of the many variables derived from the advanced whole-body MRI protocol and to create a structural and functional imaging atlas to model the aging of organs. All this information will be useful in developing advanced imaging biomarkers to identify biopsychosocial risks associated with aging and in generating new hypotheses for further study. Identifying risk factors for health problems through advanced imaging biomarkers based on whole-body MRI could help stratify subjects in the population who could benefit most from primary prevention.

Acknowledgments

The Aging Imageomics Study has been funded by Pla Estratègic de Recerca i Innovació en Salut (PERIS) 2016-2020 from the Department of Health, Generalitat of Catalonia (file number, SLT002/16/00250); and the study-dedicated 1.5T MRI scanner and ancillary MRI equipment was provided by Toshiba Medical Systems (now Canon Medical Systems). The study was partially funded by 'La Caixa Foundation. We would like to express our sincere gratitude to the Aging Imageomics Study participants for their valuable contribution. We also thank the study staff for data collection and study coordination. Albert Einstein College of Medicine owns the copyright for the Memory Binding Test and makes it available as a service to the research community but charges for commercial use (for permission requests contact the AECOM at: biotech@einstein.yu.edu); the Spanish and Catalan adaptations used were provided by the BarcelonaBeta Brain Research Center and the Pasqual Maragall Foundation with the AECOM's permission. For further information about these versions, contact Nina Gramunt at: ngramunt@pmaragall.org.

Appendix A. Supplementary data

Supplementary material related to this article can be found, in the online version, at doi:https://doi.org/10.1016/j.mad.2020.111257.

References

Bai, X., 2018. Biomarkers of aging. Adv. Exp. Med. Biol. 1086, 217–234.
Baker 3rd, G.T., Sprott, R.L., 1988. Biomarkers of aging. Exp. Gerontol. 23, 223–239.
Bamberg, F., Kauczor, H.U., Weckbach, S., et al., 2015. Whole-body MR imaging in the german national cohort: rationale, design, and technical background. Radiology 277, 206–220.
Bezerra, R.O.F., Recchimuzzi, D.Z., Dos Santos Mota, M.M., et al., 2019. Whole-body magnetic resonance imaging in the oncology setting: an overview and update on recent advances. J. Comput. Assist. Tomogr. 43, 66–75.
Bild, D.E., Bluemke, D.A., Burke, G.L., et al., 2002. Multi-ethnic study of atherosclerosis: objectives and design. Am. J. Epidemiol. 156, 871–881.
Caballero, F.F., Soulis, G., Engchuan, W., et al., 2017. Advanced analytical methodologies for measuring healthy ageing and its determinants, using factor analysis and machine learning techniques: the ATHLOS project. Sci. Rep. 7, 43955.
Caspers, S., Moebus, S., Lux, S., et al., 2014. Studying variability in human brain aging in a population-based German cohort-rationale and design of 1000BRAINS. Front. Aging Neurosci. 14 (6), 149.
Chuang, M.L., Gona, P., Salton, C.J., et al., 2012. Usefulness of the left ventricular myocardial contraction fraction in healthy men and women to predict cardiovascular morbidity and mortality. Am. J. Cardiol. 109, 1454–1458.
Clouston, S.A., Brewster, P., Kuh, D., et al., 2013. The dynamic relationship between physical function and cognition in longitudinal aging cohorts. Epidemiol. Rev. 35, 33–50.
Cole, J.H., Franke, K., 2017. Predicting age using neuroimaging: innovative brain ageing biomarkers. Trends Neurosci. 40, 681–690.
Cole, J.H., Poudel, R.P.K., Tsagkrasoulis, D., et al., 2017. Predicting brain age with deep learning from raw imaging data results in a reliable and heritable biomarker. Neuroimage 163, 115–124.
Cole, J.H., Ritchie, S.J., Bastin, M.E., et al., 2018. Brain age predicts mortality. Mol. Psychiatry 23, 1385–1392.
Cole, J.H., Marioni, R.E., Harris, S.E., Deary, I.J., 2019. Brain age and other bodily 'ages': implications for neuropsychiatry. Mol. Psychiatry 24, 266–281.
Conde-Sala, J.L., Portellano-Ortiz, C., Calvó-Perxas, L., Garre-Olmo, J., 2017. Quality of life in people aged 65+ in Europe: associated factors and models of social welfare-analysis of data from the SHARE project (Wave 5). Qual. Life Res. 26 (4), 1059–1070.
Coppola, L., Cianflone, A., Grimaldi, A.M., et al., 2019. Biobanking in health care: evolution and future directions. J. Transl. Med. 17 (1), 172.
Corominas Barnadas, J.M., López-Pousa, S., Vilalta-Franch, J., Calvó-Perxas, L., Juvinyà Canal, D., Garre-Olmo, J., 2017. MESGI50 study: description of a cohort on Maturity and Satisfactory Ageing. Gac. Sanit. 31 (6), 511–517.
Craig, C.L., Marshall, A.L., Sjostrom, M., et al., 2003. International physical activity questionnaire: 12-country reliability and validity. Med. Sci. Sports Exerc. 35, 1381–1395.
Czeyda-Pommersheim, F., Martin, D.R., Costello, J.R., Kalb, B., 2017. Contrast agents for MR imaging. Magn. Reson. Imaging Clin. N. Am. 25, 705–711.
Dafflon, J., Pinaya, W.H.L., Turkheimer, F., Cole, J.H., Leech, R., Harris, M.A., et al., 2019. Analysis of an Automated Machine Learning Approach in Brain Predictive Modelling: A Data-driven Approach to Predict Brain Age From Cortical Anatomical Measures. Cornell University, arXiv:1910.03349.
Detrano, R., Guerci, A.D., Carr, J.J., et al., 2008. Coronary calcium as a predictor of coronary events in four racial or ethnic groups. N. Engl. J. Med. 358, 1336–1345.
Engchuan, W., Dimopoulos, A.C., Tyrovolas, S., et al., 2019. Sociodemographic indicators of health status using a machine learning approach and data from the English longitudinal study of aging (ELSA). Med. Sci. Monit. 25, 1994–2001.
Erbel, R., Möhlenkamp, S., Moebus, S., et al., 2010. Coronary risk stratification, discrimination, and reclassification improvement based on quantification of subclinical coronary atherosclerosis: the Heinz Nixdorf Recall study. J. Am. Coll. Cardiol. 56, 1397–1406.
European Society of Radiology (ESR), 2015. ESR position paper on imaging biobanks. Insights Imaging 6, 403–410.
Foo, H., Mather, K.A., Thalamuthu, A., Sachdev, P.S., 2019. The many ages of man: diverse approaches to assessing ageing-related biological and psychological measures and their relationship to chronological age. Curr. Opin. Psychiatry 32, 130–137.
Franceschi, C., Garagnani, P., Morsiani, C., et al., 2018. The continuum of aging and age-related diseases: common mechanisms but different rates. Front Med (Lausanne) 12 (5), 61.
Fritz, C.O., Morris, P.E., Richler, J.J., 2012. Effect size estimates: current use, calculations, and interpretation. J. Exp. Psychol. Gen. 141, 2–18.
Gialluisi, A., Di Castelnuovo, A., Donati, M.B., de Gaetano, G., Iacoviello, L., Moli-sani Study Investigators, 2019. Machine learning approaches for the estimation of biological aging: the road ahead for population studies. Front. Med. (Lausanne) 6, 146.
Giger, M.L., 2018. Machine learning in medical imaging. J. Am. Coll. Radiol. 15, 512–520.
Golden, C.J., 1978. The Stroop Color and Word Test. Stoelting, Wood Dale, IL.
Gramunt, N., Sánchez-Benavides, G., Buschke, H., 2016. The memory binding test development of two alternate forms into Spanish and Catalan. J. Alzheimers Dis. 52, 283–293.
Hamet, P., Tremblay, J., 2017. Artificial intelligence in medicine. Metabolism 69S, S36–S40.
Hegedüs, P., von Stackelberg, O., Neumann, C., et al., 2019. How to report incidental findings from population whole-body MRI: view of participants of the German National Cohort. Eur. Radiol. 29, 5873–5878.
Hegenscheid, K., Kühn, J.P., Völzke, H., Biffar, R., Hosten, N., Puls, R., 2009. Whole-body magnetic resonance imaging of healthy volunteers: pilot study results from the population-based SHIP study. Rofo 181, 748–759.
Hertel, J., Friedrich, N., Wittfeld, K., et al., 2016. Measuring biological age via metabonomics: the metabolic age score. J. Proteome Res. 15, 400–410.
Hetterich, H., Bayerl, C., Peters, A., et al., 2016. Feasibility of a three-step magnetic resonance imaging approach for the assessment of hepatic steatosis in an asymptomatic study population. Eur. Radiol. 26, 1895–1904.
Hofman, A., van Duijn, C.M., Franco, O.H., et al., 2011. The Rotterdam Study: 2012 objectives and design update. Eur. J. Epidemiol. 26, 657–686.
Johnson, T.E., 2006. Recent results: biomarkers of aging. Exp. Gerontol. 41, 1243–1246.
Jylhävä, J., Pedersen, N.L., Hägg, S., 2017. Biological age predictors. EBioMedicine 21, 29–36.
Kroenke, K., Spitzer, R.L., Williams, J.B., 2001. The PHQ-9: validity of a brief depression severity measure. J. Gen. Intern. Med. 16, 606–613.
Kuhl, C.K., Träber, F., Gieseke, J., et al., 2008. Whole-body high-field-strength (3.0-T) MR imaging in clinical practice. Part II. Technical considerations and clinical applications. Radiology 247, 16–35.
Kühn, J.P., Hernando, D., Muñoz del Rio, A., et al., 2012. Effect of multipeak spectral modeling of fat for liver iron and fat quantification: correlation of biopsy with MR imaging results. Radiology 265, 133–142.
Kumar, V., Gu, Y., Basu, S., et al., 2012. Radiomics: the process and the challenges. Magn. Reson. Imaging 30, 1234–1248.
Kwee, R.M., Kwee, T.C., 2019. Whole-body MRI for preventive health screening: a systematic review of the literature. J. Magn. Reson. Imaging 50, 1489–1503.
Larue, R.T., Defraene, G., De Ruysscher, D., Lambin, P., van Elmpt, W., 2017. Quantitative radiomics studies for tissue characterization: a review of technology and methodological procedures. Br. J. Radiol. 90 (1070), 20160665.
Lee, K.W., Park, Y.J., Rho, Y.N., et al., 2011. Measurement of carotid artery stenosis: correlation analysis between B-mode ultrasonography and contrast arteriography. J. Korean Surg. Soc. 80, 348–354.
Lemne, C., Jogestrand, T., de Faire, U., 1995. Carotid intima-media thickness and plaque in borderline hypertension. Stroke 26, 34–39.
Lezak, M., Howieson, D., Bigler, E., Tranel, D., 2012. Neuropsychological Assessment. Oxford University Press, New York.
Martí, R., Parramon, D., García-Ortiz, L., Rigo, F., Gómez-Marcos, M.A., Sempere, I., García-Regalado, N., Recio-Rodriguez, J.I., Agudo-Conde, C., Feuerbach, N., Garcia-Gil, M., Ponjoan, A., Quesada, M., Ramos, R., 2011. Improving interMediAte risk management. MARK study. BMC Cardiovasc. Disord. 13 (11), 61.
Martínez-González, M.A., García-Arellano, A., Toledo, E., et al., 2012. A 14-item Mediterranean diet assessment tool and obesity indexes among high-risk subjects: the PREDIMED trial. PLoS One 7, e43134.
Miller, K.L., Alfaro-Almagro, F., Bangerter, N.K., et al., 2016. Multimodal population brain imaging in the UK Biobank prospective epidemiological study. Nat. Neurosci. 19, 1523–1536.
Mount, S., Lara, J., Schols, A.M., Mathers, J.C., 2016. Towards a multidimensional healthy ageing phenotype. Curr. Opin. Clin. Nutr. Metab. Care 19, 418–426.
Oakden-Rayner, L., Carneiro, G., Bessen, T., Nascimento, J.C., Bradley, A.P., Palmer, L.J., 2017. Precision Radiology: predicting longevity using feature engineering and deep learning methods in a radiomics framework. Sci. Rep. 7, 1648.
Obuchowski, N.A., Reeves, A.P., Huang, E.P., et al., 2015. Quantitative imaging biomarkers: a review of statistical methods for computer algorithm comparisons. Stat. Methods Med. Res. 24, 68–106.
Obuchowski, N.A., Buckler, A., Kinahan, P., et al., 2016. Statistical issues in testing conformance with the quantitative imaging biomarker alliance (QIBA) profile claims. Acad. Radiol. 23, 496–506.
Obuchowski, N.A., Mozley, P.D., Matthews, D., Buckler, A., Bullen, J., Jackson, E., 2019. Statistical considerations for planning clinical trials with quantitative imaging biomarkers. J. Natl. Cancer Inst. 111, 19–26.
Papp, K.V., Amariglio, R.E., Mormino, E.C., et al., 2015. Free and cued memory in relation to biomarker-defined abnormalities in clinically normal older adults and those at risk for Alzheimer's disease. Neuropsychologia 73, 169–175.
Parekh, V.S., Jacobs, M.A., 2019. Deep learning and radiomics in precision medicine. Expert Rev. Precis. Med. Drug Dev. 4, 59–72.
Petersen, S.E., Matthews, P.M., Bamberg, F., et al., 2013. Imaging in population science: cardiovascular magnetic resonance in 100,000 participants of UK Biobank – rationale, challenges and approaches. J. Cardiovasc. Magn. Reson. 15, 46.
Rammstedt, B., John, O.P., 2007. Measuring personality in one minute or less: a 10-item short version of the Big five Inventory in English and German. J. Res. Pers. 41, 203–212.
Schieda, N., Blaichman, J.I., Costa, A.F., et al., 2018. Gadolinium-based contrast agents in kidney disease: a comprehensive review and clinical practice guideline issued by the Canadian association of radiologists. Can. J. Kidney Health Dis. 5 2054358118778573.
Schlett, C.L., Hendel, T., Weckbach, S., et al., 2016. Population-based imaging and radiomics: rationale and perspective of the German national cohort MRI study. Rofo 188, 652–661.
Schmermund, A., Möhlenkamp, S., Stang, A., et al., 2002. Assessment of clinically silent atherosclerotic disease and established and novel risk factors for predicting myocardial infarction and cardiac death in healthy middle-aged subjects: rationale and design of the Heinz Nixdorf RECALL Study: risk factors, evaluation of coronary calcium and lifestyle. Am. Heart J. 144, 212–218.
Sheehan, D.V., Lecrubier, Y., Sheehan, K.H., et al., 1998. The Mini-International Neuropsychiatric Interview (M.I.N.I.): the development and validation of a structured diagnostic psychiatric interview for DSM-IV and ICD-10. J. Clin. Psychiatry 59 (Suppl 20), 22–33.
Simm, A., Nass, N., Bartling, B., Hofmann, B., Silber, R.E., Navarrete Santos, A., 2008. Potential biomarkers of ageing. Biol. Chem. 389, 257–265.

Simon, A., Gariepy, J., Chironi, G., Megnien, J.L., Levenson, J., 2002. Intima-media thickness: a new tool for diagnosis and treatment of cardiovascular risk. J. Hypertens. 20, 159–169.
Smith, A., 1982. Symbol Digit Modalities Test: Manual. Western Psychological Services, Los Angeles, CA.
Snyderman, R., 2012. Personalized health care: from theory to practice. Biotechnol. J. 7, 973–979.
Splansky, G.L., Corey, D., Yang, Q., et al., 2007. The third generation cohort of the national heart, lung, and blood institute's Framingham Heart Study: design, recruitment, and initial examination. Am. J. Epidemiol. 165, 1328–1335.
Srivastava, S., 2019. Emerging insights into the metabolic alterations in aging using metabolomics. Metabolites 9, 301.
The ARIC Investigators, 1989. The atherosclerosis risk in communities (ARIC) study: design and objectives. Am. J. Epidemiol. 129, 687–702.
Touboul, P.J., Hennerici, M.G., Meairs, S., et al., 2012. Mannheim carotid intima-media thickness and plaque consensus (2004-2006-2011). An update on behalf of the advisory board of the 3rd, 4th and 5th watching the risk symposia, at the 13th, 15th and 20th European Stroke Conferences, Mannheim, Germany, 2004, Brussels, Belgium, 2006, and Hamburg, Germany, 2011. Cerebrovasc. Dis. 34, 290–296.
Tully, P.J., Debette, S., Mazoyer, B., Tzourio, C., 2017. White matter lesions are associated with specific depressive symptom trajectories among incident depression and dementia populations: three-city dijon MRI study. Am. J. Geriatr. Psychiatry 25, 1311–1321.
Verlinden, V.J.A., van der Geest, J.N., Hofman, A., et al., 2017. Brain MRI-markers associate differentially with cognitive versus functional decline leading to dementia. J. Am. Geriatr. Soc. 65, 1258–1266.
Völzke, H., Alte, D., Schmidt, C.O., et al., 2011. Cohort profile: the study of health in Pomerania. Int. J. Epidemiol. 40, 294–307.
Wechsler, D., 1997. Wechsler Adult Intelligence Scale – Administration and Scoring Manual. Psychological Corporation, San Antonio, TX.
Wendelhag, I., Gustavsson, T., Suurküla, M., Berglund, G., Wikstrand, J., 1991. Ultrasound measurement of wall thickness in the carotid artery: fundamental principles and description of a computerized analysing system. Clin. Physiol. 11, 565–577.
Williams, A.M., Liu, Y., Regner, K.R., Jotterand, F., Liu, P., Liang, M., 2018. Artificial intelligence, physiological genomics, and precision medicine. Physiol. Genomics 50, 237–243.
Zenge, M.O., Ladd, M.E., Vogt, F.M., Brauck, K., Barkhausen, J., Quick, H.H., 2005. Whole-body magnetic resonance imaging featuring moving table continuous data acquisition with high-precision position feedback. Magn. Reson. Med. 54, 707–711.